

# Reduction of Ground Impact of a Powered Exoskeleton by Shock Absorption Mechanism on the Shank

Jeongsu Park, Daeho Lee, Kyeong-won Park and Kyoungchul Kong

**Abstract**—Powered exoskeletons for people with paraplegia are subjected to repetitive and large impacts due to the repeated ground contacts. The repetitive impact forces not only deteriorate the wear comfort but also cause a serious damage to the muscles and bones of the human wearing the powered exoskeleton. To address this issue, a novel shock absorption mechanism for powered exoskeletons that can reduce the peak of ground reaction force up to 28% is designed in this paper. The designed absorption mechanism is integrated into the WalkON Suit, a powered exoskeleton for people with paraplegia and verified by experimental results with a human subject in this paper also.

## I. INTRODUCTION

Shock absorption systems are ones of the most important elements in all mobility systems; they have been applied to most of the vehicles such as cars, motorcycles, and bicycles. The purpose of the shock absorbers includes not only improvement of the driving comfort by reducing shocks transmitted from the uneven ground, but also protecting and preventing the mechanical damage of vulnerable components from the impact force.

Powered exoskeletons are also receiving great attention as a personal mobility device for people with difficulty in walking [1], [2], [3]. The powered exoskeletons are similar to personal wheeled vehicles in many aspects. For example, both they are continuously contacting the ground, which means that both systems must be exposed to impact forces due to the unevenness of the ground. Also, the performance is examined qualitatively by the feeling of the human in the center of the device, i.e., the driver of the transportation system and the wearer of the powered exoskeleton. The requirements for the powered exoskeletons, however, may be tougher than those for the typical personal vehicles in general. The powered exoskeletons may be exposed to bigger impulses, because their feet repeatedly hit the ground while alternating the swing and stance phases to generate the repetitive walking motions. Moreover, the impact forces due to the ground contacts may cause a serious damage to the skeletal system of the wearer's body in the case of the powered exoskeleton. The impact forces are transmitted to the human body in any case, and the repeated impulses can cause bone-fatigue and even bone-fracture. Therefore, the absorption of the ground impact energy is very critical not

\*This work was supported by the Technology Innovation Program [or Industrial Strategic Technology Development Program (20003914)] funded by the Ministry of Trade, Industry and Energy(MOTIE, South Korea).

The authors are with the Department of Mechanical Engineering, Korea Advanced Institute of Science and Technology, Daejeon, Republic of Korea, 34141 e-mail: {jeongsu.park, dhlee20, kyeongwon.park, kckong}@kaist.ac.kr.



Fig. 1. WalkON Suit 4.0, the powered exoskeleton for paraplegics which is mainly utilized in this paper. (a) is the outsole module where the pressure sensor is embedded in.

only for the protection of the robot hardware but also for the safety and protection of the human body.

When the wearer of a powered exoskeleton has complete paraplegia so that he/she needs to fully rely on the powered exoskeleton for walking, the shock energy absorption during the ground impacts becomes more critical [4]. In such cases, the shock due to the ground contact is transmitted naively to the upper body of the wearer, as well as the robot frames, and the wearer must withstand these impact forces with the upper-extremity muscles [5]. To maintain the balance, the wearer needs to make extra efforts to control and hold crutches. Walking with a powered exoskeleton with the crutches for a long time, therefore, increases probability of the wrist and shoulder injuries significantly.

There have been various approaches to reduce an impact from the viewpoint of the control of actuators or the design of a gait pattern. Oh et al. developed frequency-shaped impedance control [6], [7] utilizing a disturbance observer [8] and showed that the proposed method could manipulate the impedance of robot joint at the timing of impact. Qungxuan et al. proposed a trajectory planning method for reducing the impact force of a robot joint [9]. These approaches, however, cannot be applied to the powered exoskeletons, because the mechanical impedance of joints of the powered exoskeletons cannot be lowered at any time in order to support the body weight of the wearer. In addition, the powered exoskeletons have difficulty in controlling the ground contact force and timing [10], due to the human factors, which makes reacting to the ground impact by the control of robot joints more challenging. Due to such complexity and uncertainties, it

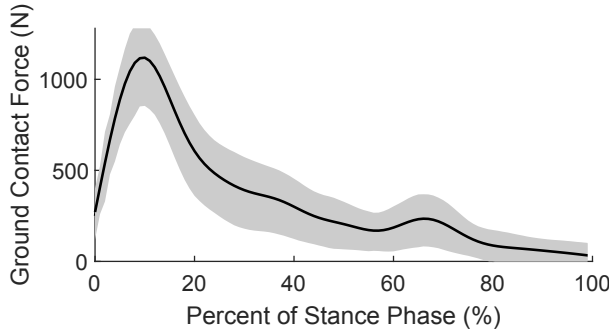


Fig. 2. The mean (line) and one-sigma standard deviation (shaded area) of ground reaction forces measured during the stance phase at the heel.

is an inherently challenging problem to manage the ground contact forces of a powered exoskeleton.

To address these issues, a mechanical shock absorption system may be necessary. There were several trials to install a suspension system to powered exoskeletons. Jun et al. installed a shock absorption mechanism on a powered exoskeleton [11], but the proposed system was bulky as it was to deal with a very large impact such as falling from high jump. Lee et al. designed a hip and knee suspension system with shape-memory-alloy springs [12], but this method was not suitable for powered exoskeletons for people with paraplegia because it cannot be applied in parallel to actuators with the high joint impedance.

In this paper, a new shock absorption system is designed for a powered exoskeleton. The proposed shock absorption system consists of a mechanical suspension system that physically absorbs the impact energy using appropriate viscoelastic elements. The proposed shock absorption system is applied to the shank of WalkON Suit [13], a powered exoskeleton for people with paraplegia. The design requirements and the resultant design parameters are introduced in this paper and verified by experimental results.

## II. DESIGN OF A SHOCK ABSORPTION MECHANISM FOR POWERED EXOSKELETON

### A. Ground Reaction Force of Powered Exoskeleton without Shock Absorption System

Fig. 2 shows the ground reaction forces measured from the outsole module of WalkON Suit 4. The outsole module (Fig. 1(a)) has air-tube coils and air-pressure sensors at the areas of the heel and the metatarsal heads. The combination of the air-tubes coils and the air-pressure sensors is the same as in our previous research [14], and thus the ground reaction forces applied to the normal direction of the outsole module can be accurately measured. As shown in Fig. 2, a large impact force is exerted at the initial contact. The magnitude of the average impact peak force at the initial contact was measured as 1100 N, and the duration of the impact force at the initial contact, i.e.,  $\Delta t_{IC}$  can be modeled as 20 percent of a gait cycle.

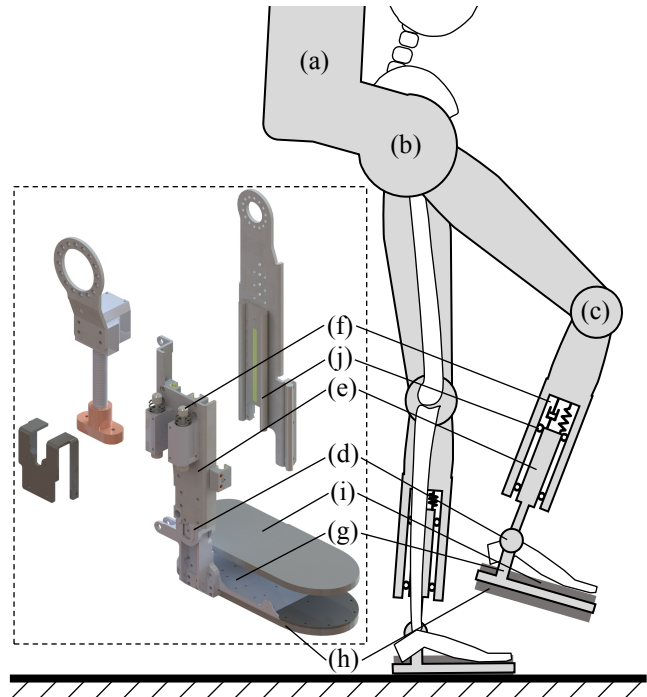


Fig. 3. The schematic of the proposed shock absorption mechanism for WalkON Suit: (a) the backpack including the electrical peripherals, (b) the hip joint actuator, (c) the knee joint actuator, (d) the ankle joint actuator, (e) the mover connected to the ankle joint and the outsole module, (f) the suspension system, (g) the outsole module, (h) the outsole cushion, (i) the insole cushion, and (j) linear guide for the mover.

### B. Design Concept of a Shank Shock Absorption Mechanism

In order to deal with impact forces transmitted from the ground, a mechanical shock absorption system is proposed, as shown in Fig. 3. The backpack system, the hip and knee joints, and the thigh frames [see (a), (b), and (c) in Fig. 3] are the same as WalkON Suit 4. However, the outsole module and the ankle joint (i.e., (d) and (g) in the figure) are separated from the shank frame, and connected to the shank frame through a suspension system [see (e) and (f) in Fig. 3]. In order to prevent bending of the tibia bones of the wearer, the suspension system is installed only in the direction parallel to the shank frame, and the other motions are prevented by a linear guide.

The spring constant,  $k$ , and the damping coefficient,  $c$ , of the suspension system, shown in Fig. 3(f), should be determined to effectively attenuate the impact force observed in Fig. 2. The design criteria for the Shank Shock Absorption Mechanism, SSAM are as follows.

- 1) When the powered exoskeleton is standing straight, the length of SSAM is minimized and length of the shank becomes  $l_{min}$ .
- 2) The length of SSAM is gradually reduced absorbing the impact energy during the ground contact.
- 3) The SSAM is fully extended and the shank length becomes  $l_{max}$  such that it is ready to absorb the impact right before the ground contact.

The first condition is preventing joint misalignments be-

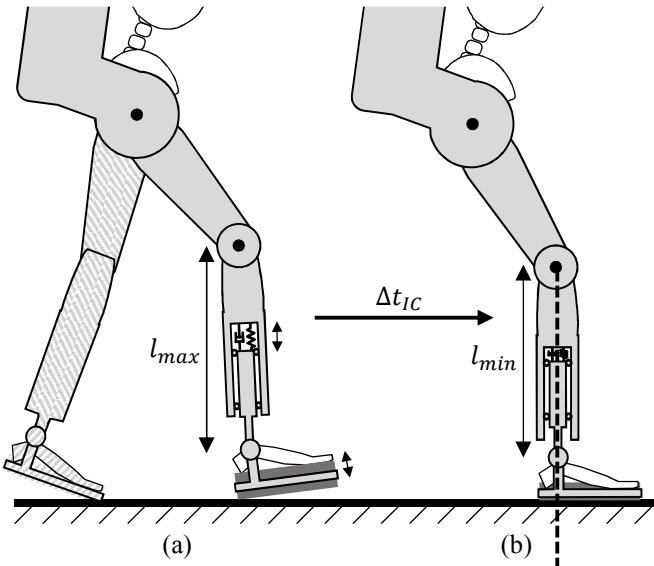


Fig. 4. Working sequence of Shank Shock Absorption Mechanism, SSAM. As mentioned in design criteria 2) and 3), (a) is the moment right before the ground impact and (b) is the moment when the absorption is finished.  $l_{max}$  is the length of the shank when the stroke of the suspension system is fully restored and  $l_{min}$  is the length of the shank when the shock is fully absorbed.

tween the exoskeleton and a wearer. Since the thigh and the shank of the wearer is fastened to the exoskeleton, misalignments of hip and knee joints between the wearer and the exoskeleton cause severe pressure to the fastened body parts [15]. Therefore, the length of the exoskeleton shank which is variable by the suspension system should always be not shorter than that of the wearer. However, it can be longer in the swing phase. Due to the fact that the outsole module [as in (d) in Fig. 3] is not fastening the wearer's body tightly and existence of the insole cushion compensates for the longer exoskeleton shank, there is no external pressure between the exoskeleton and the wearer when the shank of the exoskeleton is longer than that of the pilot on the air.

The second condition secures riding comfort of a wearer which is the objective of SSAM. Without shock absorption, the vertical velocity of the system drops abruptly to zero at the moment of the ground impact and generates jerk movements. In order to remove the jerk, the velocity of the suspension system should change gradually. To achieve that, appropriate spring constant  $k$ , damping coefficient  $c$  and pretension of the spring  $l_{pre}$  will be introduced in the following part.

The last condition ensures consistent absorbing performance under the repeating impact of walking while fully utilizing the stroke of a damper. Each length of SSAM will be reduced to the mechanical limit at the end of the stance phase due to the ground impact and the following load by the whole exoskeleton system. If SSAM fails to restore the maximum stroke during the subsequent swing phase, the next absorption would not be successful since it would reach stroke limit before the complete dissipation of the impact.

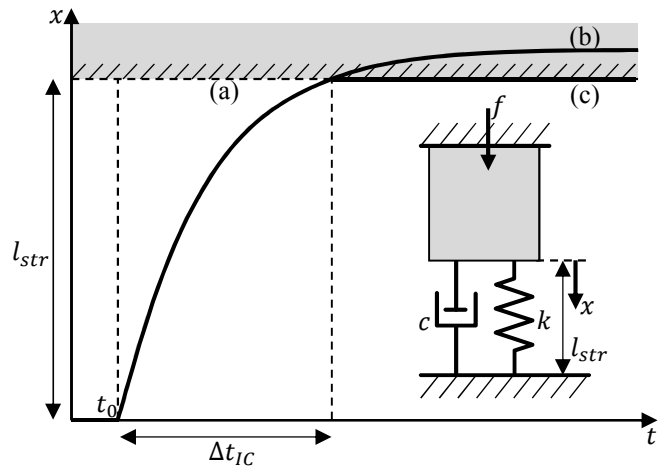


Fig. 5. The response of the proposed suspension system during a stance phase; (a) shows the mechanical limit, (b) is the ideal response according to the design criteria 2, and (c) is the actual response with the mechanical limit.

### C. Design Parameterization

Firstly, for the purpose of satisfying the design criteria 1),  $x$  should be maximally reduced while standing, an inequality is introduced with suspension stroke  $l_{str}$ , i.e.,

$$\frac{((m_{robot} + m_{human})g - f_{pre})}{2k} > l_{str}, \quad (1)$$

where  $l_{str} = l_{max} - l_{min}$ , and  $f_{pre} = k \cdot l_{pre}$

Fig. 5 shows the ideal response of the proposed suspension system during a stance phase which is suggested in design criteria 2).  $x$  and  $l_{str}$  are respectively the length and the maximum stroke of the suspension, which is determined by the distance between the mechanical stops.  $\Delta t_{IC}$  is the time interval for the suspension system to absorb the impact energy.  $t_0$  is the time when a ground contact occurs (i.e., the initial contact), and it is assumed to be zero without loss of generality.

Since it is definitely undesired that the suspension system introduces a vibration to the robotic leg, it is assumed that the suspension system is over-damped.

There are two factors that mainly affect the response of suggested over-damped system in the stance phase; force as a result of body weight, and impulse by initial contact velocity. The suspension response by the applied body weight force ( $f_{st}$ ) can be defined as  $x_{stw}(t)$ , i.e.,

$$x_{stw}(t) = \frac{f_{st}}{k} (1 - c_1 e^{-(\zeta - \sqrt{\zeta^2 - 1}) \omega_n t} + c_2 e^{-(\zeta + \sqrt{\zeta^2 - 1}) \omega_n t}), \quad (2)$$

where  $c_1 = \frac{\zeta + \sqrt{\zeta^2 - 1}}{2\sqrt{\zeta^2 - 1}}$ ,  $c_2 = \frac{\zeta - \sqrt{\zeta^2 - 1}}{2\sqrt{\zeta^2 - 1}}$ ,  $\zeta$  is the damping ratio, and  $\omega_n$  is the natural frequency.

Assume that the body weight of the wearer ( $m_{human}g$ ) and the weight of WalkON Suit ( $m_{robot}g$ ) are the forces acting on the suspension system at the initial contact, neglecting the inertial forces due to the acceleration/deceleration.

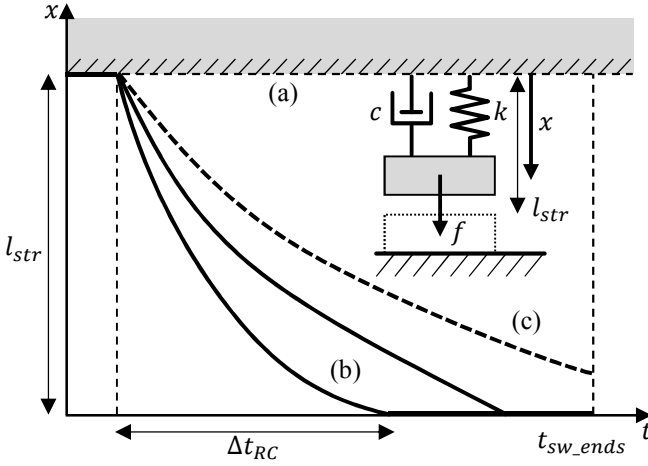


Fig. 6. The response of the proposed suspension system during a swing phase; (a) shows the mechanical limit. Solid lines (b) shows the available response while dashed line (c) is not satisfying the design criteria 3.

Introducing pretension of the spring ( $F_{pre}$ ), the magnitude of the applied force is  $f_{st} = (m_{robot} + m_{human})g - F_{pre}$ .

In addition, response by initial ground contact velocity is defined as  $x_{im}(t)$ , i.e.,

$$x_{im}(t) = c_3(e^{(-\zeta+\sqrt{\zeta^2-1})\omega_n t} - e^{(-\zeta-\sqrt{\zeta^2-1})\omega_n t}), \quad (3)$$

where  $c_3 = \frac{\hat{F}}{2m\omega_n\sqrt{\zeta^2-1}}$ .  $\hat{F}$  is impulse momentum which is determined by vertical falling velocity ( $v_0$ ) at the moment of ground contact. Assuming that  $v_0$  is fully transmitted to SSAM, this can be analyzed as an impulse response where  $\hat{F} = mv_0$

Therefore, by the principle of superposition, (2) and (3) can be utilized to determine displacement of suspension in the stance phase  $x_{st}(t)$ . In order to follow the design criteria 2), at  $t = \Delta t_{IC}$ ,  $x(t)$  should be less than the maximum length. Therefore design criteria 2) can be summarized into one equation.

$$x_{st}(\Delta t_{IC}) = x_{stw}(\Delta t_{IC}) + x_{im}(\Delta t_{IC}) < l_{max} \quad (4)$$

At last, to fulfill the design criteria 3), in the short moment of swing, spring has to overcome the damper as shown in Fig. 6. Two main factors that results in response of the suspension system is force applied by swing foot weight and initial displacement of the suspension resulted by previous stance phase. Response by the force is defined as  $x_{sww}(t)$ , and it can be expressed as

$$x_{sww}(t) = \frac{f_{sw}}{k}(1 - c_1 e^{-(\zeta-\sqrt{\zeta^2-1})\omega_n t} + c_2 e^{-(\zeta+\sqrt{\zeta^2-1})\omega_n t}), \quad (5)$$

where  $c_1$  and  $c_2$  is same in (2), but the applied force is  $f_{sw} = -m_{foot}g - F_{pre}$ . During the swing phase, dynamic model is different from the stance phase. Moving object is foot and applied force  $m_{foot}g$  has same direction with the spring pretension force.

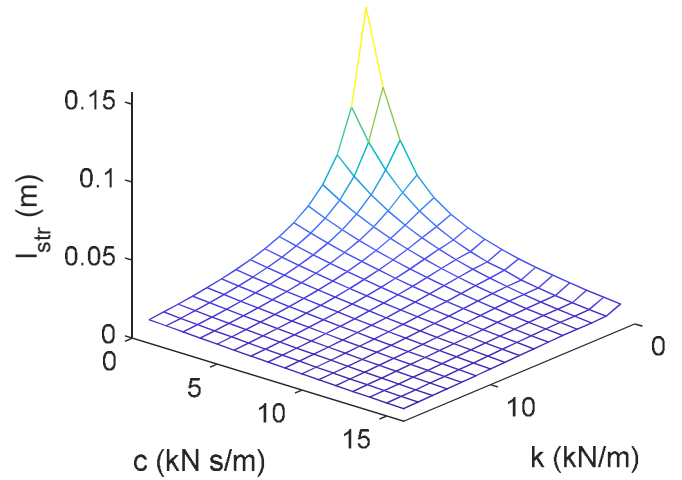


Fig. 7. Available set of design variable  $k$ ,  $c$  and corresponding  $l_{str}$  under the condition of  $l_{pre} = 0.003m$

Besides, response by initial displacement is defined as  $x_{id}(t)$ , and it can be described as

$$x_{id}(t) = c_4 e^{(-\zeta+\sqrt{\zeta^2-1})\omega_n t} + c_5 e^{(-\zeta-\sqrt{\zeta^2-1})\omega_n t}, \quad (6)$$

where  $c_4 = x_{sw}(0) \left( \frac{\zeta+\sqrt{\zeta^2-1}}{2\sqrt{\zeta^2-1}} \right)$  and  $c_5 = x_{sw}(0) \left( \frac{-\zeta+\sqrt{\zeta^2-1}}{2\sqrt{\zeta^2-1}} \right)$ .

Assuming under the toughest condition ( $x_{sw}(0) = l_{str}$ ), displacement of the suspension in the swing phase have to reach 0 before  $\Delta t_{step}$ . For recover time shorter than step period,  $\Delta t_{RC} < \Delta t_{step}$ , below equation has to be satisfied.

$$x_{sw}(\Delta t_{RC}) = x_{sww}(\Delta t_{RC}) + x_{id}(\Delta t_{RC}) = 0 \quad (7)$$

To faithfully follow the objective of SSAM, a set of  $k$ ,  $c$  and  $F_{pre}$  that satisfies all three equation (1), (4), and (7) should be selected. Fig. 7 shows a set of available constant  $k$  and damping coefficient  $c$  and corresponding suspension stroke  $l_{str}$  under pretension of 0.003m which is an arbitrarily selected value within the range that is easy to implement.

### III. IMPLEMENTATION OF SHANK SHOCK ABSORPTION MECHANISM INTO A POWERED EXOSKELETON

#### A. Parameter Selection

From the available design variable set in Fig. 7 which is calculated under condition of system weight  $m_{robot} + m_{human} = 100kg$  and initial ground contact velocity  $v_0 = 0.12m/s$ , realizable set was selected as  $l_{str} = 0.012m$ ,  $k = 15000N/m$ ,  $c = 2700Ns/m$ , and  $l_{pre} = 0.003m$ . By applying two spring - damper system in parallel, those variables can be implemented to the narrow space on the shank of WalkON Suit 4.

#### B. Assembly of Shank Shock Absorption Mechanism

As shown in Fig. 8, SSAM is largely classified into three components. Fig. 8(a), the shank lateral frame, consists of lead screw and screw nut which is designed for length adjusting to fit the exoskeleton into any individual pilot. Fig.

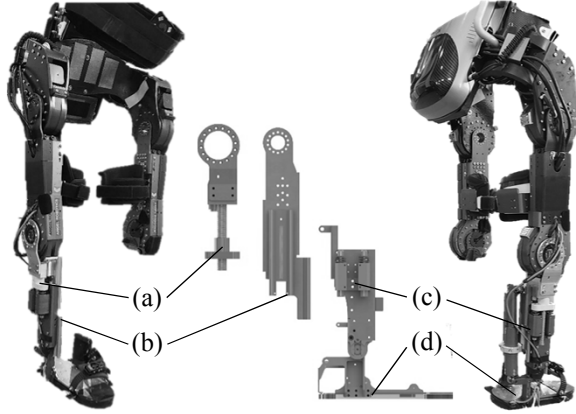


Fig. 8. Manufactured components of shank shock absorption mechanism applied to the WalkON Suit: (a) shank lateral frame, (b) shank medial frame, (c) the suspension system, and (d) the outsole module.

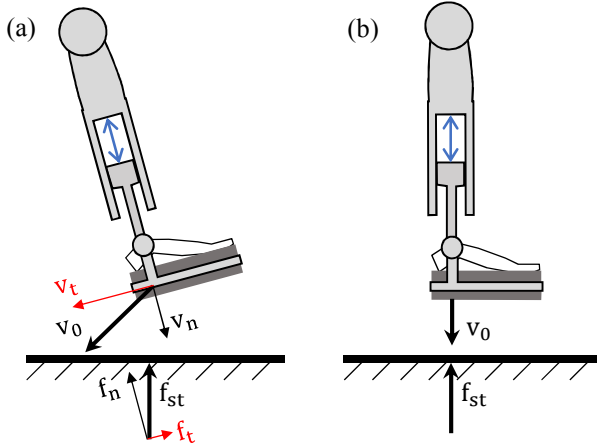


Fig. 9. Forces acting on the shank shock absorber at the initiation of stance.  $v_t$ ,  $v_n$ ,  $f_n$  and  $f_t$  represents tangential and normal component of contact velocity  $v_0$  and stance force  $f_{st}$  described on Section II-C. (a) shows remaining impacts when shock absorber is not aligned with the impact while (b) shows vertical contact condition which fully absorbs the impacts.

8(b), the shank medial frame, consists of three rails which act as linear guides and enable relative movements to part (c). Fig. 8(c) consists of five rail blocks which is linked with Fig. 8(b) and spring - damper system designed in Section II. Pressure sensor and electric ledger is embedded in Fig. 8(d) to evaluate the ground reaction force.

### C. Gait Pattern

In consideration of a piston type absorption system which absorbs parallel directional shocks, there would be remaining shocks if SSAM is not aligned with the ground impact. Assuming that the ground impact caused by the body weight is perpendicular to the surface of the ground, stance would initiate vertically to the ground so as to align the absorbing direction and impact direction from body weight; the direction of the gravitational acceleration.

As mentioned on Section II-C, the impulse occurs also from the initial contact velocity,  $v_0$  in (3), velocity vector of  $v_0$  should also be aligned with the absorption system.

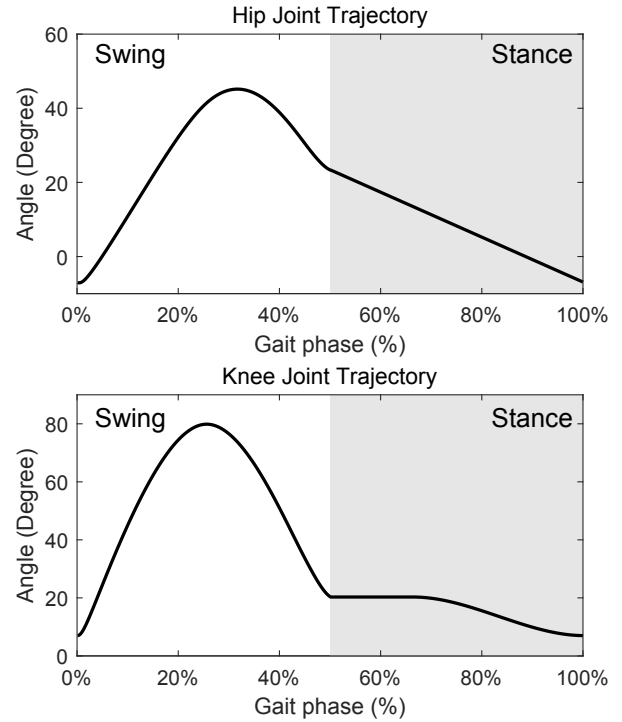


Fig. 10. Predefined joint trajectory of the proposed gait pattern to maximize the shock absorption performance. The angle represents the flexion angle of each joint.

Otherwise, there would be remaining shocked caused by  $v_t$  and  $f_t$  in Fig. 9(a), which cannot be absorbed.

To compromise consistent shock absorbing performance for every step, predefined trajectory of Fig. 10 is used repeatedly with phase difference of 50% between left and right leg. This joint trajectory ensures alignment between absorption mechanism and the impact from body weight and initial velocity. Ankle joint is not described in details because it is weakly related with the initial ground contact impact.

Fig. 10, the predefined joint trajectory, is generated under condition of thigh length 0.354m and shank length 0.380m. Since the joint trajectory is completely parameterized, it can be applied even if the user changes.

## IV. PERFORMANCE EVALUATION

### A. Experimental Setup

SSAM implemented WalkON Suit 4 was used for evaluation. Calibrated air pressure sensor in our previous research [14] is embedded in the outsole module in Fig. 8(d) to evaluate the absorbing performance of the proposed mechanism. A pilot of 75kg wears WalkON Suit 4 and firstly walked with proposed absorption system. Subsequently, by using stroke stopper, pilot walked with suspension system locked. To observe the changes of the ground reaction force according to the presence of the proposed absorption system, all the other settings kept in same condition.

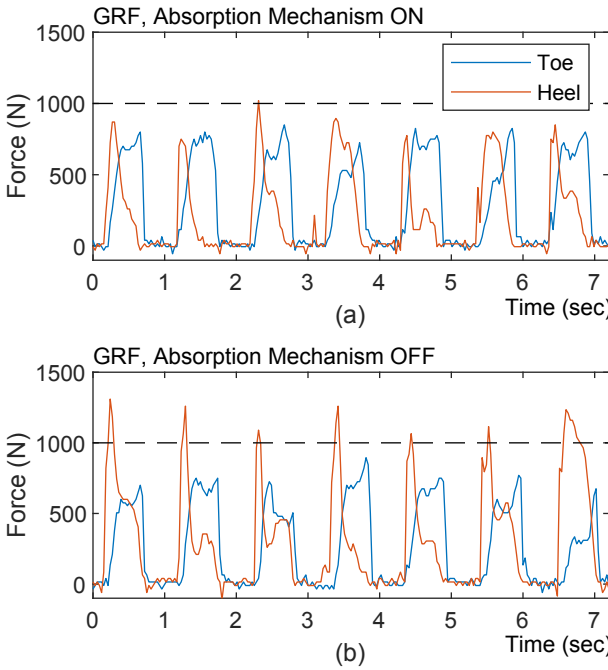


Fig. 11. GRF obtained from sensor embedded in outsole. (a) the GRF data with absorption mechanism and (b) without absorption mechanism.

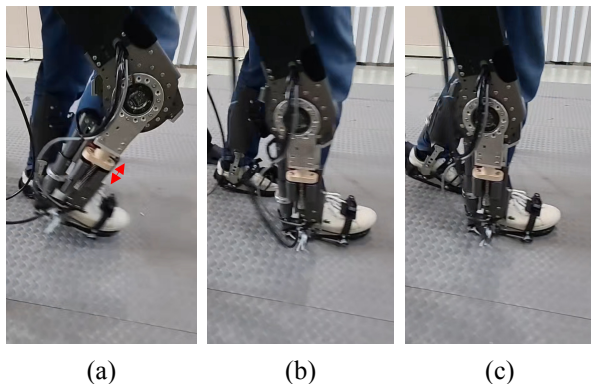


Fig. 12. Video capture of shank shock absorber mechanism working sequence; (a) restoring maximum stroke before ground contact. Length of shank should finalizes to  $l_{max}$ . (b) length of SSAM reducing gradually absorbing ground impacts. (c) finish of absorbing as stroke of SSAM is fully used. shank length finalized to  $l_{min}$ .

### B. Verification of Absorption Performance

Fig. 11(a) is GRF measured at the heel and toe when the absorption mechanism is working. Zero force section can be analyzed as swing phase, e.g. 0.75s to 1.1s. As the heel strikes the ground at the start of the stance phase and the toe push off the ground at the end of the stance phase, GRF of heel reaches the peak value before the GRF of toe reaches the peak value. Comparing Figs. 11(a) and (b), mean peak value of the heel GRF has decreased 342N, 28% while toe GRF remains the same. It can be concluded that the ground impact at the start of stance phase has been absorbed by implementing proposed absorption mechanism.

### V. CONCLUSION AND FUTURE WORK

In this paper, it was confirmed that the peak value of the GRF reduced 28% (342N) by attaching proposed absorption mechanism, SSAM, to the powered exoskeleton, WalkON Suit 4.0. As a result, It is obvious that the jerk movement has decreased. For our next step, prevention of human injuries such as bone fatigue and increased durability of exoskeleton will be measured by additional sensors with various pilots and lengthened evaluation time.

### REFERENCES

- [1] Rewalk robotics. [Online]. Available: <http://rewalk.com>
- [2] Ekso bionics. [Online]. Available: <http://eksobionics.com>
- [3] Angel robotics. [Online]. Available: <http://angel-robotics.com/>
- [4] F. H. M. van Herpen, van R. B. Dijsseldonk, H. Rijken, N. L. W. Keijzers, J. W. K. Louwerens, and I. J. W. van Nes, "Case report: Description of two fractures during the use of a powered exoskeleton," *Spinal Cord Series and Cases*, vol. 5, no. 1, p. 99, Dec 2019.
- [5] A. J. Smith, B. N. Fournier, J. Nantel, and E. D. Lemaire, "Estimating upper extremity joint loads of persons with spinal cord injury walking with a lower extremity powered exoskeleton and forearm crutches," *Journal of Biomechanics*, vol. 107, p. 109835, 2020. [Online]. Available: <http://www.sciencedirect.com/science/article/pii/S002192902030258X>
- [6] S. Oh, H. Woo, and K. Kong, "Frequency-shaped impedance control for safe human–robot interaction in reference tracking application," *IEEE/ASME Transactions on Mechatronics*, vol. 19, no. 6, pp. 1907–1916, 2014.
- [7] S. Oh, K. Kong, and Y. Hori, "Design and analysis of force-sensor-less power-assist control," *IEEE Transactions on Industrial Electronics*, vol. 61, no. 2, pp. 985–993, 2014.
- [8] T. Umeno and Y. Hori, "Robust speed control of dc servomotors using modern two degrees-of-freedom controller design," *IEEE Transactions on Industrial Electronics*, vol. 38, no. 5, pp. 363–368, 1991.
- [9] J. Qingxuan, L. Tong, C. Gang, S. Hanxu, and Z. Jian, "Trajectory optimization for velocity jumps reduction considering the unexpectedness characteristics of space manipulator joint-locked failure."
- [10] K. Park, J. Park, J. Choi, and K. Kong, "Adaptive gait pattern generation of a powered exoskeleton by iterative learning of human behavior," unpublished.
- [11] J. Ueda, M. Turkseven, E. Kim, Q. Lowery, C. Bivens, and M. Mayo, "Shock absorbing exoskeleton for vertical mobility system: Concept and feasibility study," 10 2018, pp. 3342–3349.
- [12] S. Lee, S. Lee, Y. Na, B. Ahn, H. Jung, S. S. Cheng, N. Kim, T.-S. Jun, and Y. Kim, "Shock absorber mechanism based on an sma spring for lightweight exoskeleton applications," *International Journal of Precision Engineering and Manufacturing*, vol. 20, no. 9, pp. 1533–1541, Sep 2019. [Online]. Available: <https://doi.org/10.1007/s12541-019-00169-y>
- [13] J. Choi, B. Na, P. Jung, D. Rha, and K. Kong, "Walkon suit: A medalist in the powered exoskeleton race of cybathlon 2016," *IEEE Robotics Automation Magazine*, vol. 24, no. 4, pp. 75–86, 2017.
- [14] K. Kong and M. Tomizuka, "A gait monitoring system based on air pressure sensors embedded in a shoe," *IEEE/ASME Transactions on Mechatronics*, vol. 14, no. 3, pp. 358–370, 2009.
- [15] D. Zanotto, Y. Akiyama, P. Stegall, and S. Agrawal, "Knee joint misalignment in exoskeletons for the lower extremities: Effects on user's gait," *IEEE Transactions on Robotics*, vol. 31, pp. 978–987, 08 2015.